IRSTI 43.03.51 https://doi.org/10.26577/ijmph.20251613

Zhumagulov A.[1], Serebryanskiy A.[1], Reva I.[1] and Voropaev V.[2]

[1]Fesenkov astrophysical institute, 050020, Observatory 23, Almaty, Kazakhstan
[2]Keldysh Institute of Applied Mathematics, Miusskaya sq., 4, Moscow, 125047, Russia
*e-mail: zhumagulov@fai.kz
(Received 10 April 2025; revised 28 May 2025; accepted 5 June 2025)

Statistical Analysis of the Situation in Geostationary Orbits

Abstract. This study uses statistical analysis to examine near-miss events (NME) in geostationary earth orbit (GEO) from 2011 to 2024. The analysis is based on orbital propagation derived from GEO orbital element catalogs and observational data of events. Results show an overall increase in NMEs, which can be attributed to new satellite launches and better space debris fragment detection. The average daily distribution of NMEs is not symmetrical longitudinally; more events happen at 75°E longitude than at 255°E. However, potentially dangerous NMEs within 10 km are more common at 255°E. The relationship between the average daily number of events and the minimum object separation changes over time. From 2011 to 2024, daily dangerous NMEs within 1 km increased from 0.24 to 0.39 events/day. Based on a 20-meter collision threshold, the 2024 data suggests a potential collision event in geostationary orbit every eight years. If current trends continue, collisions in GEO could happen every six years by 2030 and every four years by 2040.
Keywords: Space debris, Near-Earth Space, Geostationary orbit, Near-Miss Events, Space situational awareness.

Introduction

The Near-Earth Space (NES) environment is experiencing a continuous increase in the number of artificial satellites deployed annually. Data from Celestrak [https://celestrak.org/satcat/boxscore.php], as of mid-March 2025, indicates a total of 30,116 cataloged objects in near-Earth space, comprising 11,448 active satellites and 15,672 inactive objects classified as space debris. Space debris can persist in Earth's orbit for extended periods. In low Earth orbit, orbital decay occurs due to atmospheric drag, facilitating a degree of self-cleaning. In contrast, geostationary orbit presents a significantly different scenario, with objects capable of remaining for very long durations, while achieving linear velocities up to 4 km/sec.

A primary risk within the NES environment is the operational failure of satellites resulting from collisions with fragments of space debris. The velocity of these fragments renders even those smaller than 1 cm in diameter a considerable hazard, capable of causing damage to critical satellite components and potentially leading to complete functional loss. Debris objects exceeding 10 cm in size present an almost certain probability of causing the catastrophic destruction of the spacecraft.

While isolated small fragments do not present a substantial hazard, their vast quantity and erratic trajectory render them exceedingly perilous. Consequently, continued space exploration may become untenable, as an unchecked proliferation of space debris could precipitate the Kessler syndrome [1]. This phenomenon involves spacecraft collisions generating escalating amounts of debris, thereby significantly augmenting the likelihood of further destruction.

Many papers and reviews have been dedicated to the examination of the environment within NES [2,3,4,5], with a particular emphasis on the geostationary orbit regime [6,7,8,9,10]. Observational activities targeting NES objects have been continuously undertaken at the Fesenkov Astrophysical Institute (FAI) since the launch of the first satellites in 1957. For multiple decades, the geostationary orbit has been subject to systematic surveillance, enabling the compilation of a GEO catalog [11]. This has further facilitated a statistical analysis of the GEO environment, drawing upon five catalogs spanning the period from 2000 to 2013 [6]. The analysis led to the conclusion that the issue of space debris and near-miss events involving satellites in geostationary orbits is escalating in urgency. It was further posited that, absent the

adoption of refined methodologies for collision control and prevention, the associated risks will inevitably be amplified.

The study by [7] significantly broadened the analysis of the GEO environment using 81 FAI catalogs from 2011 to 2020. The results of their research indicate that in 2020, spacecraft encounters within 200 meters happened approximately every 50 days, and a collision in GEO could be anticipated every 8 years.

The FAI is improving the SSA(Space situational awareness) regional system in Kazakhstan by observing and forecasting NMEs daily. Over 500 observations of such events were conducted between 2020 and 2024. This paper presents a statistical analysis of both NME observations and the GEO situation from 2011 to 2024, based on 137 updated GEO catalogs available in the FAI database.

Materials and Methods

The material used for the analysis

The FAI's GEO catalog is subject to continuous updates, incorporating data obtained through collaborative agreements and memoranda with partner institutions, as well as data derived from systematic observations conducted by FAI facilities situated at the Assy-Turgen and Tien-Shan Observatories. The GEO catalog experiences continuous expansion due to several factors: the deployment of new satellites, the proliferation of space debris fragments (for instance due to the Intelsat 33e destruction incident), and advancements in detection technology and methodologies that enable the identification of progressively smaller objects. Fig.1 illustrates the annual variation in the number of objects presented in the FAI catalogues. The average number of objects in 2011 is assumed to be the zero reference level. The errors in the Fig.1 correspond to the standard deviation of the number of objects for each year. It is worth emphasizing that the increase in the number of objects in the catalogs cannot be fully explained only by the increase in the number of annual launches on the GEO. This trend is described by linear dependence [10]:

$$\Delta N = 0{,}62 \cdot x - 1218, \qquad (1)$$

where x is the date in years. In Fig. 1, the values of ΔN are shown by a red dashed line. As shown in Fig. 1, a precipitous decline in the rate of catalog object growth occurred in 2020, followed by an absolute reduction in the number of objects in 2021. The increase was subsequently restored post-2022. This phenomenon may be attributed to a reduction in tracked objects resulting from the COVID-19 pandemic. This observation elucidates the potential for mass epidemics to exert an indirect influence upon NES security.

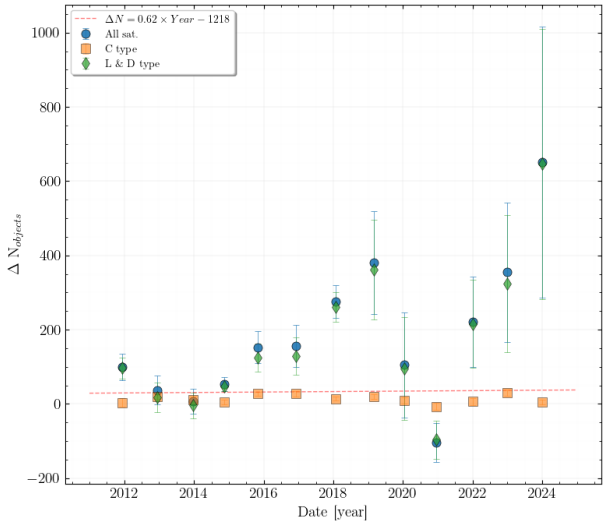

Figure 1 – The difference in the average number of objects in GEO catalogs, depending on the epoch of a catalog and type of objects (C-controlled, L-librating, D-drifting).

Statistical analysis of observed NMEs

While the accuracy of orbital calculations using catalog data has been and remains a research topic [12,13,14,15], these works often focus on evaluating the accuracy of satellite state vector calculations. However, when predicting near-miss events, the accuracy of determining mutual distances and the moment of closest approach is more critical than the accuracy of individual satellite position and velocity calculations. This accuracy depends on the presence of systematic and random errors in calculations and may be better or worse than the accuracy of state vector calculations. To assess the accuracy of NME forecasts, we compared the parameters of the predicted events with those obtained from observations of these events.

Since the absolute distance between the objects can not be directly measured from angular observations alone, we use the error of minimum angular distance, $\Delta u(E) = \min |u_o - u_c|$, as a proxy to estimate the precision of absolute distance calculations. Here E represents the epoch of the forecast in days before the event, u_o is the observed minimum angular distance, and u_c is the predicted minimum angular distance. This assumption is justified because the error in determining the position of an object in orbit propagation is maximal along the track. Therefore, the moment of closest approach is the moment of minimum angular distance, which generally differs from the moment of minimum absolute distance. The accuracy of determining the moment of the minimum angular distance is $\Delta t(E) = \min |t_o - t_c|$.

The analysis used results of NME observations conducted at FAI between January 17, 2020, and February 23, 2025. A total of 532 NMEs were observed during this period: 136 events in 2020, 123 in 2021, 42 in 2022, 133 in 2023, 79 in 2024, and 19 events in the first two months of 2025. Observations were limited to events where the predicted minimum absolute distance between objects one day prior to the event was less than 30 km.

The precision of forecasting is influenced by errors in determining the moment of closest approach and the corresponding minimum angular distance between objects. These errors are primarily caused by observation conditions, which are determined by the quality of the atmosphere, as measured by the seeing parameter. At the Tien-Shan Observatory, the median seeing range of 2.0-2.5 arcseconds translates to roughly 500 meters of linear angular distance for topocentric distances to the geostationary region.

The dependency of the average values of $\Delta u(E)$ and $\Delta t(E)$ on the forecast epoch, E, is illustrated in Fig. 2. These average values were calculated from a total of 532 events, with the standard deviation representing the error of the average.

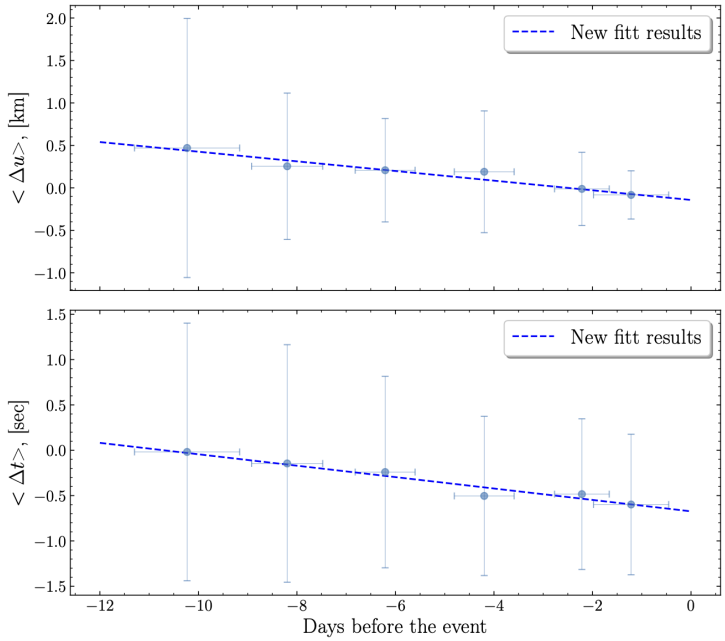

Figure 2 – The accuracy of event time (<Δt(E)>) and minimum angular distance (<Δu(E)>) forecasts changes depending on the number of days before the event.

Fig. 2 illustrates that the systematics in forecasting NMEs depend on the catalog's epoch, and the error increases with epoch. While this dependence of the systematic can be factored into NME forecasts, it introduces an error of approximately 10 km for predictions made 120 days before the event. The error increase, on the other hand, translates to roughly 14 km in terms of angular distance $\Delta u(E = 120)$, is substantial for precise forecasting but should not significantly impede statistical analysis. It should be noted that when analyzing observed NME, the method we use to determine the extremum of the dependence of the mutual angular distance between objects has a lower accuracy in determining the precise time of event. This is partly explained by the fact that when the satellites move slowly with respect to each other, the true time of the minimum of the angular distance is difficult to determine. This systematics may also be present in the dependence shown in Figure 2 for Δt(E).

Statistical analysis of predicted NMEs

The forecast was performed for all NMEs with an absolute distance between objects ranging from 1 to 200 km. The statistical analysis of near-miss events at GEO was based on 120-day forecast results. The reasoning for selecting this forecast duration can be found in [7].

Fig. 3 and Fig. 4 display the change in the average daily number of events, n(R), at distances up to 200 km, 100 km, 50 km, and 25 km from 2011 to 2024, based on analysis of the FAI catalogues. As in the previous work, we use the empirical dependence of the average daily number of NMEs on the distance between objects:

$$n(R) = \gamma \cdot R^{\beta}, \tag{2}$$

or,

$$lg\, n(R) = \alpha + \beta lgR, \tag{3}$$

where $\alpha = lg\, \gamma$. The dependence of the average daily number of NMEs in geostationary orbits, n(R), on the absolute distance R, between satellites from 2011 to 2024 (Fig. 5). The analysis of this dependence allows to draw the following conclusions:

1. The number of NMEs consistently increases over time.
2. The rate at which the number of events increases over time is weakly dependent on the relative distance between objects.
3. The nature of the dependence changes approximately at a distance of 25 km.

The latter conclusion is explained, on one hand, by an increase in errors at distances of less than 25 km, since the number of such events decreases within the predicted time interval (120 days). On the other hand, at large values of R, the saturation effect begins to manifest itself (approaching the asymptotic limit).

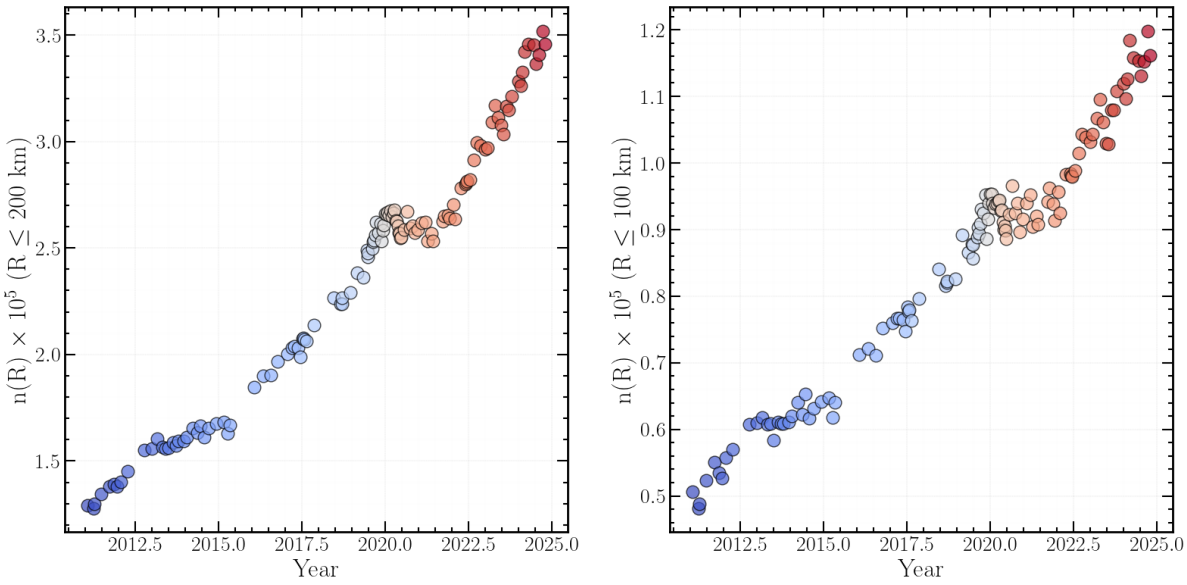

Figure 3 – The average daily number of NMEs, n(R), at distances up to 200 km (left) and up to 100 km (right) in the period from 2011 to 2024 according to the results of the FAI catalog analysis.

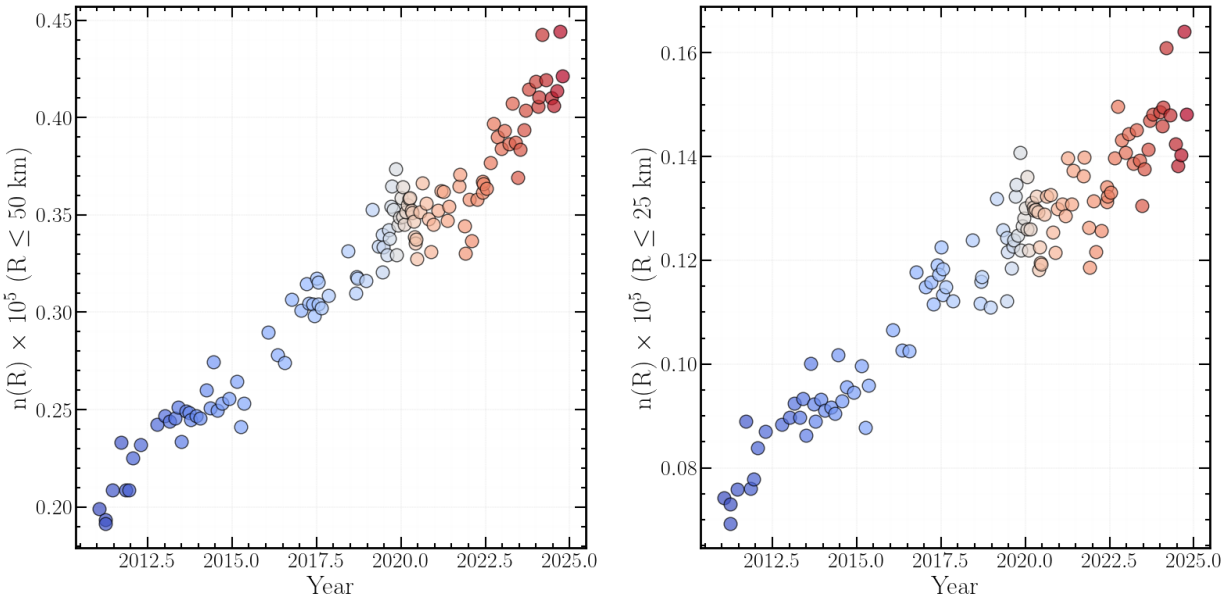

Figure 4 – The average daily number of NMEs, n(R), at a distance of up to 50 km (left) and up to 25 km (right) in the period from 2011 to 2024 according to the results of the FAI catalog analysis.

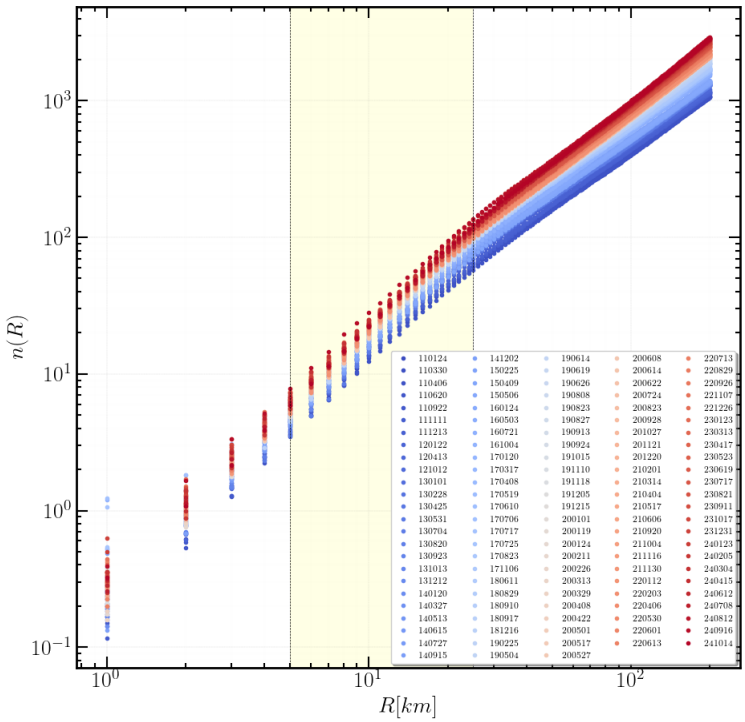

Figure 5 – The dependence of the average daily number of NMEs in geostationary orbits, n(R), on the absolute distance R, between satellites from 2011 to 2024.

Fig. 6 and Fig. 7 display the results of the distribution of the average daily number of NMEs up to certain distances, depending on the longitude over which such an event occurs. Fig. 6 and Fig. 7 shows that two regions associated with libration points, 75°E and 255°E, have the highest number of near-miss events. The total number of events at longitude 75°E is noticeably higher than at longitude 255°E.

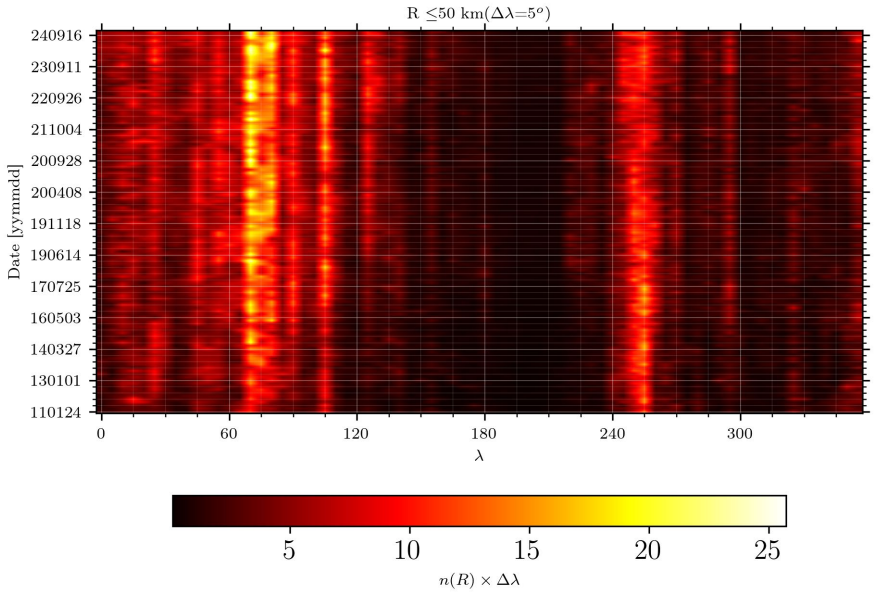

Figure 6 – The density of the average daily number of NMEs at distances up to 50 km in geostationary orbits from 2011 to 2024, depending on the longitude of the point over which such an event occurred.

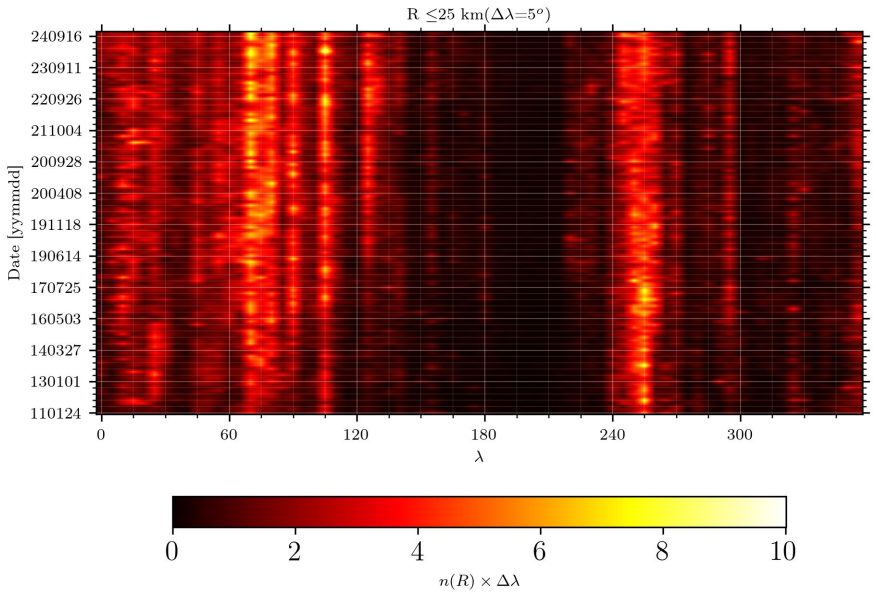

Figure 7 – The density of the average daily number of NMEs at distances up to 25 km in geostationary orbits from 2011 to 2024, depending on the longitude of the point over which such an event occurred.

To investigate the distinct behaviors of n(R) within the eastern and western hemispheres, the average daily number of NMEs was analyzed separately within the longitudinal ranges of 60°-120° and 240°-300° (Fig. 8, Fig.9).

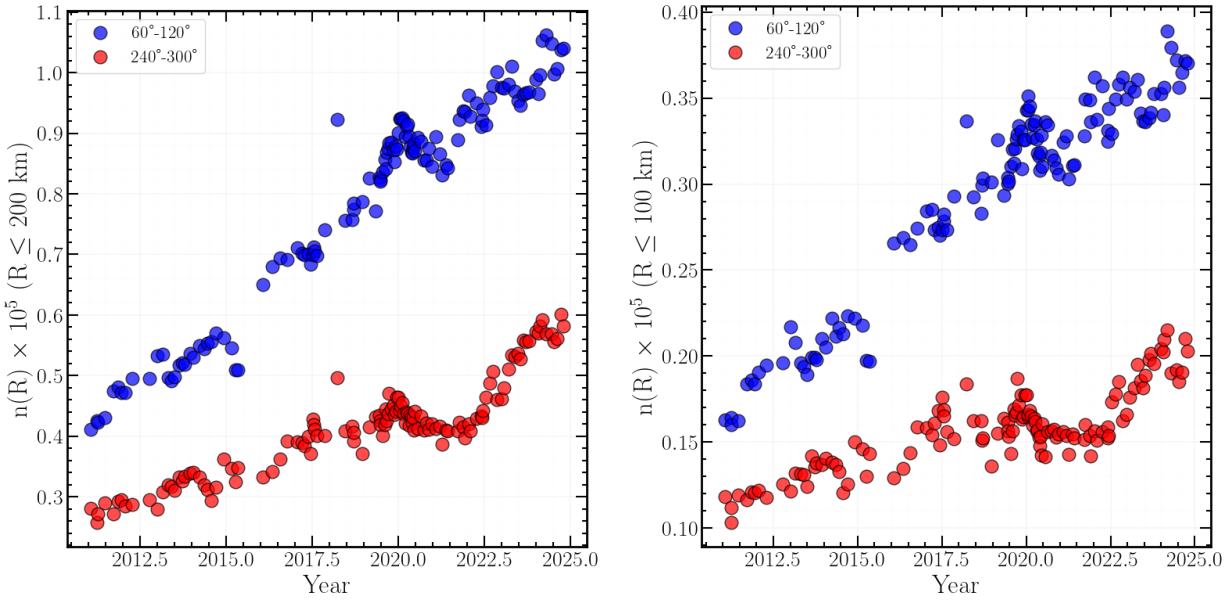

Figure 8 – The average daily number of events, n(R), at a distance of up to 200 km (left) and up to 100 km (right) in the period from 2011 to 2024 according to FAI catalog analysis. The blue dots indicate n(R) for the range 60°-120°, the red dots for the range 240°-300°.

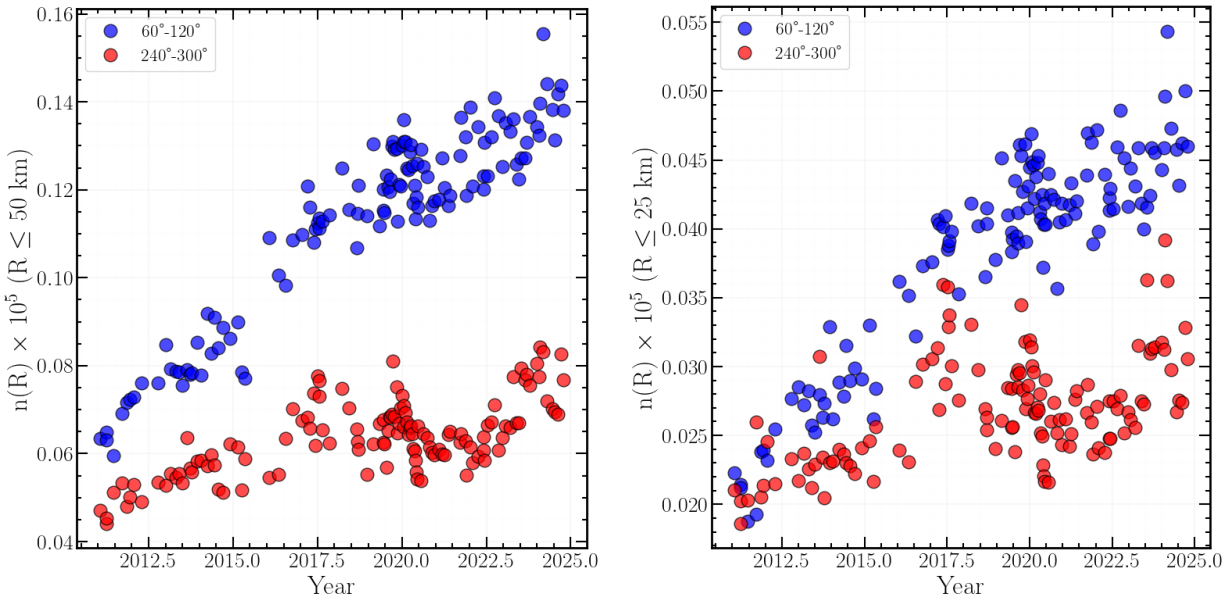

Figure 9 – The average daily number of NMEs, n(R), at a distance of up to 50 km (left) and up to 25 km (right) in the period from 2011 to 2024 according to FAI catalog analysis. The blue dots indicate n(R) for the range 60°-120°, the red dots for the range 240°-300°.

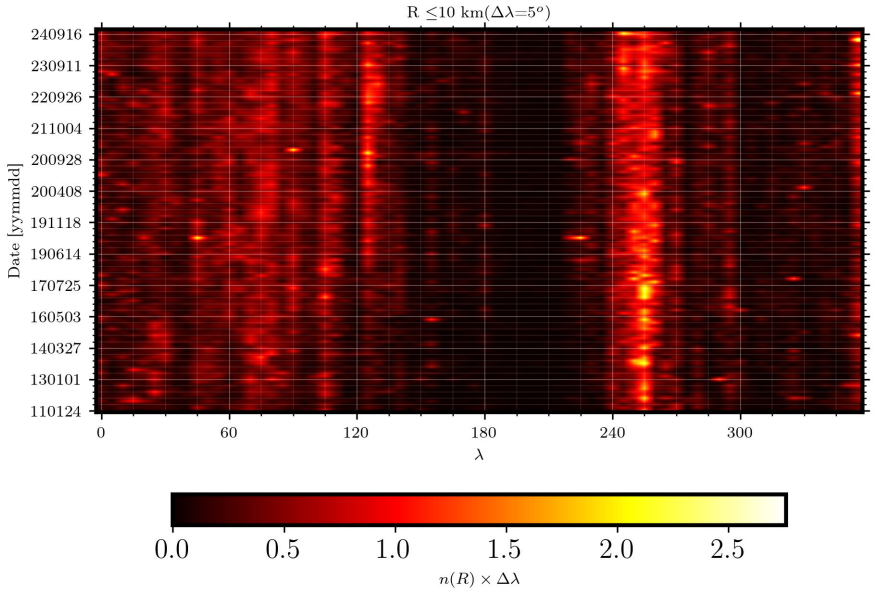

Figure 10 – The density of the average daily number of NMEs at distances up to 10 km in geostationary orbits from 2011 to 2024, depending on the longitude of the point over which such an event occurred.

Analysis of near-miss events at distances of 10 km and below is of particular importance. Given the accuracy of forecasts and observations, such distances are considered potentially hazardous, as the statistics of these events may include actual collisions between satellites. Consequently, a discrete analysis of these events was undertaken (Fig. 10). While the overall frequency of approaches may be elevated within the 60°-120° range, the density of hazardous approaches is demonstrably greater within the 240°-300° range, specifically in a restricted band proximal to longitude 255°E. From this, it can be inferred that the risk of collisions at longitude 255°E may surpass that at longitude 75°E. This observation merits further investigation and requires corroboration using independent catalogs and methodologies.

To ensure safety within the GEO, the analysis of close approach statistics at extremely close distances, indicative of potential collision events, is paramount. To evaluate these statistics, equation (3) is employed for a distance range of 5 km to 25 km, as was done in previous research. The selection of the lower limit is predicated on the requirement for statistically significant data and the precision of predictive models. The upper limit is determined by maintaining the linear relationship of equation (3). Table 1 presents the annual values of the parameters α and β. Fig. 11 illustrates the temporal dependence of these parameters. As observed in Fig. 11, the coefficient β exhibits minimal variation over time, corroborating previous findings. The magnitude of this parameter is contingent upon the selected range of distances for analysis. Consequently, to enhance the accuracy of determining the coefficient α (as well as $\gamma = 10^{\alpha}$), a subsequent iteration fixed the parameter β to its weighted mean value across the entire period, β^{-} = 1.7915 ± 0.0007. This value demonstrates a negligible discrepancy from the value reported in [7], β^{-} = 1.779 ± 0.001. A repetition of the linear approximation of dependence (3), with the coefficient β held constant, yielded refined values for the coefficients α and γ, as presented in Table 2 and shown in Fig. 12.

Table 1 -The average values of the coefficients α and β obtained from linear approximation.

DATE	α	β	DATE	α	β
2011	-0.6325 ± 0.0047	1.7582 ± 0.0044	2018	-0.4700 ± 0.0037	1.7717 ± 0.0035
2012	-0.5454 ± 0.0055	1.7405 ± 0.0048	2019	-0.4796 ± 0.0019	1.7830 ± 0.0018
2013	-0.5548 ± 0.0037	1.7563 ± 0.0035	2020	-0.4924 ± 0.0019	1.8116 ± 0.0018
2014	-0.6034 ± 0.0032	1.8016 ± 0.0029	2021	-0.4791 ± 0.0025	1.8174 ± 0.0023
2015	-0.4906 ± 0.0049	1.6921 ± 0.0052	2022	-0.4258 ± 0.0025	1.7848 ± 0.0024
2016	-0.4841 ± 0.0047	1.7453 ± 0.0044	2023	-0.4278 ± 0.0025	1.7960 ± 0.0023
2017	-0.4653 ± 0.0032	1.7675 ± 0.0030	2024	-0.4696 ± 0.0025	1.8327 ± 0.0023

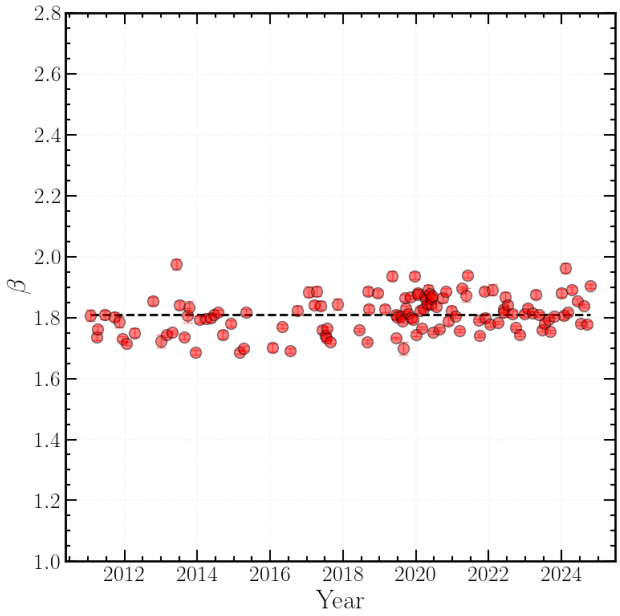

Figure 11 – The values of the coefficient β based on the analysis of the values of n(R) for the distance in the range from 5 km to 25 km.

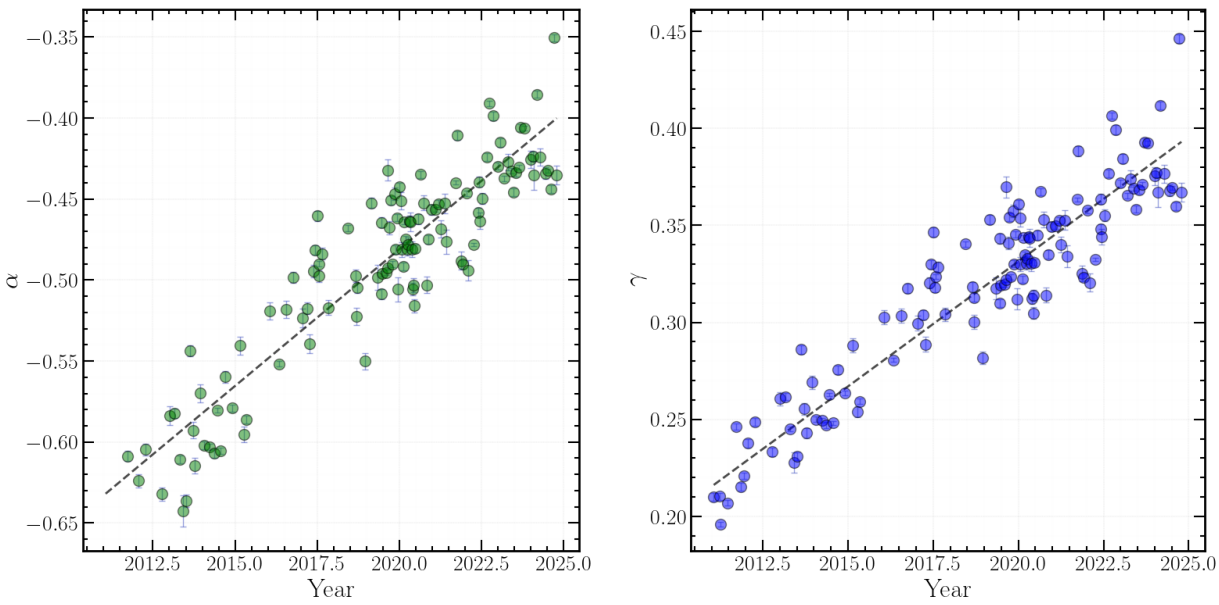

Figure 12 – On the left: the parameter α determined using a fixed value β from the results of the FAI catalog analysis. On the right: the values of the parameter γ – the average daily number of NMEs at a distance of 1 km. The results of the NMEs analyzed in the range from 5 km to 25 km. The dotted lines show the results of the linear approximation.

Table 2 – The values of α and γ obtained using the average value of β^{-} = 1.7915 ± 0.0007

DATE	α	γ	DATE	α	γ
2011	-0.6351	0.2370	2018	-0.5030	0.3140
2012	-0.6113	0.2447	2019	-0.4868	0.3259
2013	-0.5906	0.2566	2020	-0.4746	0.3352
2014	-0.5746	0.2663	2021	-0.4568	0.3593
2015	-0.5609	0.2748	2022	-0.4396	0.3634
2016	-0.5409	0.2878	2023	-0.4217	0.3787
2017	-0.5236	0.2995	2024	-0.4058	0.3928

Results and Discussion

To estimate the number of average daily events at certain distances R in a given epoch E, we rewrite the expression (3) as:

$$n_E(R) = 10^{\alpha(E)+\underline{\beta} lgR}, \qquad (4)$$

where β^{-} – the weighted mean value over all catalogs, α(E) is the value from the linear approximation listed in Table 2.

The precision in satellite position determination via ground-based optical observations is primarily dictated by the atmospheric seeing, yielding an approximate accuracy of 1 arcsecond. For the geostationary orbit, this angular error translates to a linear distance of approximately 200 meters. Consequently, establishing this value as the critical separation threshold for satellite conjunction events, with a coefficient β^{-} of 1.7915 ± 0.0007 for the epoch E, we can derive the mean daily rate of such potential collisions:

$$n_E(0.2) = 10^{\alpha(E)-1.2522} \qquad (5)$$

Based on the data in Table 2, the mean daily number of close approaches in 2011 is $n_{2011}(0.2) \approx 0.01296$, corresponding to approximately one close approach at a distance of 200 meters every 77 days. Similarly, the mean daily number of close approaches in 2020 was $n_{2020}(0.2) \approx 0.01876$, indicating approximately one approach every 53 days. Furthermore, in 2024, the mean daily number of close approaches is $n_{2024}(0.2) \approx 0.02198$, or approximately one approach at a distance of 200 meters every 45 days.

Furthermore, considering the average spacecraft dimensions, a distance of approximately 20 meters may be defined as a potential collision threshold. Consequently, with β = 1.7915, equation (3) becomes:

$$n_E(0.02) = 10^{\alpha(E)-3.044} \qquad (6)$$

Based on the 2011 catalog, the potential frequency of spacecraft collisions in GEO is estimated to be one event per 13 years. Subsequent analyses in 2020 and 2024 indicated an increased frequency, with estimations of once per 9 years and once per 7.7 years, respectively. Should this statistical trend of critical spacecraft approaches persist, projections suggest that by 2030, spacecraft collisions may occur once every 6 years, and further, once every 4 years by 2040. If we compare these forecasts with the forecasts of our previous work [7], we can see the difference. This is because the accuracy of studying the orbits of objects in our catalogs has become noticeably better, which has also affected our forecasts. An overview of the estimated frequency of potential spacecraft collisions in GEO for different epochs is provided in Table 3.

Table 3 – Frequency of spacecraft collisions at GEO by epoch.

DATE (year)	$t_{collision}$ (years)	DATE (year)	$t_{collision}$ (years)
2011	13	2020	9.0
2012	12.4	2021	8.7
2013	11.8	2022	8.3
2014	11.4	2023	8.0
2015	11.1	2024	7.7
2016	10.5	2030	6.2
2017	10.1	2040	4.2
2018	9.7	2050	2.8
2019	9.3		

The statistical analysis of near-miss events in geostationary orbit from 2011 to 2024, using FAI's GEO catalogs, reveals several critical trends. The anomalous decline in cataloged objects in 2020-2021, potentially linked to the COVID-19 pandemic, highlights the vulnerability of space surveillance activities to the global pandemic.

The analysis of observed NMEs confirms that the accuracy of forecasting these events is dependent on the catalog epoch. While systematic errors can be factored into predictions, they introduce a notable uncertainty, particularly for forecasts made far in advance. This suggests that short-term forecasts are more reliable for immediate collision avoidance maneuvers.

Fig. 3 and Fig. 4 demonstrate a consistent increase in the average daily number of NMEs over time, across various distance thresholds. This trend underscores the growing congestion in GEO and the escalating risk of collisions.

The longitudinal distribution of NMEs, shown in Fig. 6 and Fig. 7, indicates a higher overall number of events at 75°E, compared to 255°E. However, the greater density of dangerous approaches (below 10 km) at 255°E, as depicted in Fig. 10, indicates a higher risk of possible collisions in that region. This asymmetry in risk distribution warrants further investigation.

Conclusion

An analysis of the temporal dependence of Near-Miss Event frequency leads to the following conclusions: should the current rate of uncontrolled object accumulation in geostationary orbit persist, the probability of conjunctions within a 20-meter threshold (treated as a collision) is projected to be one event every six years by 2030, every four years by 2040, and every three years by 2050. This projection pertains to the entirety of the geostationary region. In regions around the libration points at longitudes 75° E and 255° E, the risk of near-miss events may be substantially elevated. The highest frequency of potentially hazardous approaches within a 10-kilometer range may manifest at longitude 255° E.

Overall, the results confirm the increasing risk of collisions in GEO due to space debris. The observed trends necessitate the development and implementation of enhanced collision avoidance strategies and international cooperation to mitigate the risks and ensure the long-term sustainability of space activities in GEO.

Acknowledgements

This research is funded by the Science Committee of the Ministry of Science and Higher Education of the Republic of Kazakhstan (Grant No. BR21881880). The FAI engineers and observers are gratefully acknowledged for their efficient and dedicated work in obtaining valuable observations of geostationary satellites and supporting FAI's optical system to regularly observe the geostationary region and update information about objects in GEO.

References

1. Kessler, D. J., N. L. Johnson, J-C Liou, and M. Matney. 'The Kessler Syndrome: Implications to Future Space Operations \(AAS 10-016\)'. In *Rocky Mountain Guidance and Control Conference, ADVANCES IN THE ASTRONOMICAL SCIENCES*, 137:47–62. San Diego, Calif.: Published for the American Astronautical Society by Univelt;, 2010. https://www.tib.eu/de/suchen/id/BLCP%3ACN078974007.

2. Adushkin, V. V., O. Yu Aksenov, S. S. Veniaminov, S. I. Kozlov, and V. V. Tyurenkova. 'The Small Orbital Debris Population and Its Impact on Space Activities and Ecological Safety'. *Acta Astronautica* 176 (November 2020): 591–97. https://doi.org/10.1016/j.actaastro.2020.01.015.

3. Pelton, Joseph N. 'A Path Forward to Better Space Security: Finding New Solutions to Space Debris, Space Situational Awareness and Space Traffic Management'. *The Journal of Space Safety Engineering* 6, no. 2 (June 2019): 92–100. https://doi.org/10.1016/j.jsse.2019.04.005.

4. Mariappan, Amrith, and John L. Crassidis. 'Kessler's Syndrome: A Challenge to Humanity'. *Frontiers in Space Technologies* 4 (November 2023): 1309940. https://doi.org/10.3389/frspt.2023.1309940.

5. Vasile, Massimiliano. 'Preface: Space Environment Management and Space Sustainability'. *Advances in Space Research*72, no. 7 (October 2023): 2443–44. https://doi.org/10.1016/j.asr.2023.07.068.Anderson, Paul V., and Hanspeter Schaub. 'Local Debris Congestion in the Geosynchronous Environment with Population Augmentation'. *Acta Astronautica* 94, no. 2 (February 2014): 619–28. https://doi.org/10.1016/j.actaastro.2013.08.023.

6. A. V. Didenko. 'Some statistical characteristics of the dangerous rapprochements in geostationary zone. (Russian)'. *NEWS OF THE NATIONAL ACADEMY OF SCIENCES OF THE REPUBLIC OF KAZAKHSTAN* 283, no. 3 (2012): 32–36. http://rmebrk.kz/journals/199/fizmat%20(3).pdf.

7. Serebryanskiy, A., Ch Akniyazov, B. Demchenko, A. Komarov, Ch Omarov, I. Reva, M. Krugov, and V. Voropaev. 'Statistical Analysis of Object Congestion in the Geostationary Region'. *Acta Astronautica* 182 (May 2021): 424–31. https://doi.org/10.1016/j.actaastro.2021.02.014.

8. Sato, Kota, Yasuhiro Yoshimura, Toshiya Hanada, Taku Izumiyama, and Ryu Shinohara. 'The Collision Avoidance Strategy for Geostationary Satellites Considering Orbit Maintenance'. *Journal of Space Safety Engineering* 8, no. 4 (2021): 331–38. https://doi.org/10.1016/j.jsse.2021.08.004.

9. Shu, Peng, Meng Zhao, Zhen-Yu Li, Wei Sun, Yu-Qiang Li, and Ya-Zhong Luo. 'Short-Term Evolution and Risks of Debris Cloud Stemming from Collisions in Geostationary Orbit'. *Acta Astronautica* 228 (2025): 486–93. https://doi.org/10.1016/j.actaastro.2024.12.016.

10. Anderson, Paul V., and Hanspeter Schaub. 'Local Debris Congestion in the Geosynchronous Environment with Population Augmentation'. *Acta Astronautica* 94, no. 2 (February 2014): 619–28. https://doi.org/10.1016/j.actaastro.2013.08.023.

11. Didenko, A., B. Demchenko, and L. Usoltseva. *Zone Catalogue of Geostationary Satellites. Issue 2*. Almaty:Gylym, 2000. http://lfvn.astronomer.ru/report/0000030/cover.htm.

12. Flohrer, T., H. Krag, and H. Klinkrad. 'Assessment and Categorization of TLE Orbit Errors for the US SSN Catalogue'. In *Advanced Maui Optical and Space Surveillance Technologies Conference*, edited by C. Paxson, H. Snell, J. Griffin, K. Kraemer, S. Price, M. Kendra, and D. %P E37 Mizuno, E53, 2008.

13. Dong, Wei, and Zhao Chang-yin. 'An Accuracy Analysis of the SGP4/SDP4 Model'. *Chinese Astronomy and Astrophysics* 34, no. 1 (2010): 69–76. https://doi.org/10.1016/j.chinastron.2009.12.009.

14. Yim, Hyeonjeong. 'Enhancement of Collision Probability Accuracy Using Improved Orbit Predictions Method'. In *SpaceOps 2012 Conference*, 2012. https://doi.org/10.2514/6.2012-1275488.

15. Früh, Carolin, and Thomas Schildknecht. 'Accuracy of Two-Line-Element Data for Geostationary and High-Eccentricity Orbits'. *Journal of Guidance, Control, and Dynamics* 35, no. 5 (2012): 1483–91. https://doi.org/10.2514/1.55843.

Information about authors:

Zhumagulov, Aslan – M.Sc, Junior Researcher, Fesenkov Astrophysical Institute, Almaty, Kazakhstan, email: zhumagulov@fai.kz

Serebryanskiy, Alexandr – Dr., Senior Researcher, Fesenkov Astrophysical Institute, Almaty, Kazakhstan, email: serebryanskiy@fai.kz

Reva, Inna – M.Sc, Senior Researcher, Fesenkov Astrophysical Institute, Almaty, Kazakhstan, email: reva@fai.kz

Voropaev, Viktor – Lead engineer, Keldysh Institute of Applied Mathematics, Moscow, Russia, email: voropaev@keldysh.ru